ELSEVIER

Polymer 42 (2001) 9111–9120

polymer

www.elsevier.com/locate/polymer

Kinetic and mechanistic details of the vesicle-to-rod transition in aggregates of PS_{310}-*b*-PAA_{52} in dioxane–water mixtures

Susan E. Burke, Adi Eisenberg*

Department of Chemistry, Otto Maass Chemistry Building, McGill University, 801 Sherbrooke Street West, Montreal, Que., Canada H3A 2K6

Received 26 February 2001; accepted 13 April 2001

Abstract

The kinetics and mechanism of the transformation of vesicular aggregates, prepared from the asymmetric, amphiphilic block copolymer polystyrene-*b*-poly(acrylic acid) in dioxane–water mixtures, into rod-like structures are investigated using turbidity measurements and transmission electron microscopy. Since the architecture of these aggregates is known to depend upon the solvent composition, small jumps in the dioxane content are used to induce the transformation. The transition proceeds with a conservation of the aggregation number. This process involves two steps, beginning with the quick collapse of the vesicles into a 'bowtie' structure. This is followed by a slow rearrangement as each bowtie forms a 'dumbbell' aggregate and finally a smooth rod. The relaxation times associated with this morphological change are found to depend upon the initial solvent composition, the magnitude of the dioxane jump, and the initial polymer concentration.

Keywords: Block copolymer aggregates; Morphological transition; Kinetics and mechanism

1. Introduction

Asymmetric, amphiphilic, block copolymers form a variety of self-assembled structures in solution; the properties of these aggregates, both under equilibrium conditions and after quenching, have been extensively investigated [1–8]. Block copolymer aggregates are most commonly spherical in shape. Micelles with a core radius that is much smaller than the cross-sectional area of the corona are referred to as star-like. de Gennes predicted that it should be possible to form micelles with a larger core radius relative to the length of the corona [9]. Halperin et al. were the first to use the phrase 'crew-cut' to describe these aggregates [10]. For block copolymer in solution, in general, the ability to form aggregates prompted several attempts to characterize the self-assembly process in such systems. It has been shown that block copolymer micelles, as in the case of small molecule surfactants, are formed through a stepwise association [11–15]. The mechanism of block copolymer self-assembly involves two steps and is similar to that proposed by Aniansson and Wall to describe micelle formation from surfactant molecules [16]. The first step involves the fast exchange of the copolymer chains between the micelles and the bulk solution. The rate-determining process includes a series of stepwise events during which copolymer molecules associate with or dissociate from the micelles.

Zhang and Eisenberg showed that crew-cut aggregates of a range of morphologies are obtained in solution from one block copolymer family [17]. This is also observed for a single block copolymer [18]. The materials that were used include asymmetric polystyrene-*b*-poly(acrylic acid) (PS-*b*-PAA) and polystyrene-*b*-poly(ethylene oxide) copolymers [17–22]. Several other block copolymers have been found to self-assemble into aggregates of multiple morphologies [23–33]. Block copolymer aggregates with different architectures have been prepared from a single polymer in solution by altering such factors as the solvent composition [34–36], the relative block lengths [37–39], the temperature [40–42], and the presence of additives [43–49]. These tunable parameters have an influence on the size and shape of the aggregates because they affect the balance between three of the major forces acting on the system. These include the stretching of the core-forming blocks, the inter-corona interactions, and the interfacial energy between the solvent and the micellar core. This force balance has a strong influence on the thermodynamics governing the equilibrium morphology of these aggregates [20,50–52].

* Corresponding author. Tel.: +1-514-398-6934; fax: +1-514-398-3797.
E-mail address: adi.eisenberg@mcgill.ca (A. Eisenberg).

0032-3861/01/$ - see front matter
PII: S0032-3861(01)00385-8

A continual increase in the perturbation imposed upon the system leads to a progressive change in both the size and shape of the block copolymer aggregates. Shen and Eisenberg have prepared a morphological phase diagram for the ternary system PS_{310}-*b*-PAA_{52}/dioxane/water [18]. They have shown that a gradual increase in the water content of the solvent mixture transports the aggregates from a region of purely spherical micelles to a solvent composition region where spheres coexist in equilibrium with rods, to a region where only rods exist, followed by a region of rod and vesicle coexistence, and then finally to a region where all of the aggregates are converted to vesicles. They have also proven that the morphological transitions are reversible by decreasing and subsequently increasing the dioxane content [18].

The conversion of vesicles to rods is the topic of the present study. In order to understand why this phenomenon occurs, it is important to consider the factors that are involved in the stabilization of vesicular structures. Although the equilibrium nature of polymer vesicles is a controversial subject, Shen and Eisenberg proposed that PS_{310}-*b*-PAA_{52} vesicles are under equilibrium control within a water content range of 28.0–40.0 wt% [18]. Since the stability of the vesicles is dependent upon the degree of stabilization of the curvature on either side of the bilayer, they predicted that the differential pressure that maintains the curvature is balanced, as the water content is increased, by the segregation of the polydisperse corona chains within the bilayer, with the long chains on the outside and the shorter chains on the inside. Recently, this hypothesis of Shen and Eisenberg was confirmed [53]. It was shown that the copolymer molecules with shorter hydrophilic block lengths do indeed segregate to the inside of the vesicle, while chains with longer hydrophilic blocks are located in the outer layer of the vesicle. This distribution of chain lengths increases the corona repulsion on the outside of the vesicles relative to that on the inside; therefore, chain segregation results in thermodynamic stabilization of the curvature.

Disturbing the equilibrium stabilization mechanism of vesicular aggregates leads to structural transformations. Although this phenomenon has been observed for vesicles formed from block copolymers [18,20,54–56], as well as other colloidal systems [57–65], the mechanistic details involved in the structural transition have only been thoroughly investigated for lipid and double-chain surfactant vesicles [57–65]. In both these cases, the vesicles are most commonly transformed into spherical micelles. The vesicle-to-micelle transformation induced by the addition of micelle-forming surfactants (e.g. octylglucoside, sodium cholate, $C_{12}E_8$, Triton X-100, hexadecyltrimethylammonium chloride, and sodium alkyl sulfates) to vesicles composed of phospholipids such as egg yolk lecithin and dipalmitoylphosphatidylcholine progress through a series of lipid–surfactant mixed assemblies formed at different molar ratios of surfactant to lipid [57–62]. However, the pathway (intermediate aggregate structures) for the transition can be very different in each case. For example, with large uniform vesicles of egg lecithin, the successive addition of ocylglucoside causes the breakdown of the vesicles to elongated tubules and small vesicles, then to open vesicles and long cylindrical aggregates, and finally to spherical micelles [58]. The use of sodium cholate to induce the vesicle-to-micelle transition in egg lecithin aggregates causes the transition to proceed through the formation of open vesicles, which are transformed to bilayer sheets. The sheets are then converted to cylindrical aggregates, and the further addition of surfactant leads to the formation of spherical micelles [61]. It must be noted that cylindrical aggregates have never been observed as intermediate structures during the vesicle-to-micelle transition induced by the addition of single-chain surfactants to solutions of vesicles formed from double-chain surfactants [63–65]. Instead, small vesicles, broken vesicles, large multi-layer lamellae vesicles, bilayer sheets, and small discs have been observed in these cases.

Despite the existence of numerous reports regarding the mechanism of vesicle breakdown in different colloidal systems, few studies address the kinetics associated with these structural transitions. Farquhar et al. investigated the kinetics and mechanism of the breakdown of sodium 6-phenyltridecane sulfate vesicles, in aqueous sodium chloride solutions, by rapid mixing of the surfactant system with a salt solution that is injected using a stop-flow device equipped with ultraviolet-visible detection [63]. The transition occurs within a time range of 0.1–10 s and involves a three-step mechanism. The vesicles are first transformed into unstable bilayer structures in the slow step. The bilayers are quickly converted into smaller disc aggregates, which rapidly dissociate to individual surfactant molecules. Brinkmann et al. used the same procedure to study the vesicle-to-micelle transition in sodium 6-phenyltridecane sulfate aggregates, in aqueous sodium chloride solutions, induced by the addition of sodium dodecyl sulfate (SDS) [65]. The structural transformation involves first-order kinetics and proceeds through a phase in which the SDS molecules interact with the vesicles. The rate constant is strongly dependent upon the concentration of SDS, decreasing from $k_{exp} = 0.090\ s^{-1}$ at 0.65 mM SDS to $k_{exp} = 0.023\ s^{-1}$ at 0.55 mM SDS.

There have been a few studies of the kinetics of morphological transitions in block copolymer aggregates, but only one of these studies involved vesicular structures [66–68]. Chen et al. investigated the kinetics and mechanism of the rod-to-vesicle transition occurring in aggregates formed from PS_{310}-*b*-PAA_{52} in dioxane–water mixtures [67]. The transition was induced with a jump in the water content of the solvent mixture. The kinetics was followed by measuring the solution turbidity as a function of time, and the intermediate aggregates were monitored with transmission electron microscopy (TEM). Near the morphological phase boundary, the rods become shorter and plumper, and vesicles start to appear in the solution. An increase in the

water content increases the population of vesicles at the expense of the rod population. The transition mechanism is believed to involve two steps. During the fast step, the short rods are flattened forming irregular or circular bowl-shaped lamellae. The slow process is the closure of the bowl-shaped lamellae to produce vesicles. The two relaxation times have been found to depend on both the initial water content and the polymer concentration, increasing with an increase in either parameter. However, the size of the water jump is found to have little influence on the transition kinetics [67].

Here, we extend the study of Chen et al. with an investigation of the kinetics and mechanism of the vesicle-to-rod transition in aggregates prepared from PS_{310}-*b*-PAA_{52} in dioxane–water mixtures. The morphological transformation is brought about by a sudden jump in the dioxane content of the solvent mixture near the boundary between the vesicle and vesicle–rod regions of the phase diagram. Turbidity measurements are used to follow the transition kinetics as a function of time. The intermediate aggregates are isolated by dropping the solution temperature to near that of liquid nitrogen, followed by warming under vacuum to freeze-dry the aggregates, which are subsequently observed using TEM. The kinetics is investigated as a function of the initial water content, the magnitude of the dioxane jump, and the initial polymer concentration. The results are compared with those obtained for the rod-to-vesicle transition [67].

2. Experimental

The block copolymer employed in this study is a polystyrene-*b*-poly(acrylic acid) [PS-*b*-PAA] sample that contains 310 PS and 52 PAA repeat units and has a polydispersity of 1.05 [52]. The polymer was prepared by sequential anionic polymerization; the details of this procedure were outlined in previous publications [69,70]. The copolymer sample was fractionated, using a standard procedure, to remove any homopolymer [17]. This fractionation process first involved the conversion of the acrylic acid blocks to sodium acrylate with the addition of sodium hydroxide to a solution of the copolymer in THF. This led to the self-assembly of the copolymer molecules into reverse micelles with a poly(sodium acrylate) core. The addition of water to the solution resulted in phase separation. The upper solution contained the homopolymer, and the above process was repeated several times until homopolymer was not detected, by gel permeation chromatograpy, in the reverse micelle phase. The sodium acrylate blocks were converted back to the acylic acid form upon treatment with hydrochloric acid and then precipitated from solution and dried under vacuum.

Aggregates with a particular morphology were prepared by first dissolving the copolymer in dioxane, which is a solvent favorable for both blocks. The copolymer molecules were driven to self-assemble with the slow addition of water (0.2 wt%/min) to the system. The appearance of a blue tint in the solution indicated the formation of micelles. The water addition was continued until the desired solvent composition was reached.

For the study of solution turbidity as a function of polymer concentration, water was added to a solution of the polymer dissolved in dioxane until the solvent was composed of 40.0 wt% water. This solution was placed in a dialysis bag (Spectra/Por) with a molecular cut-off of 8000 g/mol and dialyzed against distilled water for four days in order to remove the dioxane. The morphology of the aggregates was kinetically frozen as a result of the dialysis process. The stock solution, after dialysis, had a concentration of 3.44 wt% polymer. Several other samples with varying polymer concentration were prepared by diluting the stock solution with water. The solution turbidity was measured at 650 nm using a Varian Cary 50 spectrometer. The experiments were done at room temperature.

The morphological transition was induced by the quick addition of dioxane to the system. A change in the size and shape of the aggregates resulted in a change in the turbidity of the solution. The kinetics of the transition was monitored by following the optical density of the transmitted light (180°) as a function of time at 650 nm and at room temperature.

TEM was performed using a Phillips EM400 microscope operating at an acceleration voltage of 80 kV. The EM copper grids used to mount the sample were first coated with a thin film of poly(vinyl formal) and one of carbon. The grids were placed on a metal block, which was kept in thermal equilibrium with liquid nitrogen. A drop of the polymer solution was deposited onto the cold grids at various time points throughout the morphological transition. The samples were then dried under vacuum for 24 h. Some of the sample grids were shadowed with a palladium/platinum alloy at an angle of ca. 36° so that details about the height of the aggregates could be obtained. The dimensions of the aggregates were determined from the TEM negatives using a calibration map prepared from measurements taken of PS latex standards [20].

3. Results and discussion

3.1. Transition region and aggregate dimensions

Chen et al. have indicated in their study of the rod-to-vesicle transition that the major part of this transformation occurs above a water content of ca. 26.0 wt% and that only vesicles are observed above a water content of 27.6 wt% [18]. They consider the water content range of 25.9–27.6 wt% to be the transition zone at a polymer concentration of 1.0 wt%. At the beginning of the transition region, very few (ca. $< 5\%$) of the aggregates are present as vesicles. The location of these boundaries shifts to solvent compositions with smaller water content as the polymer

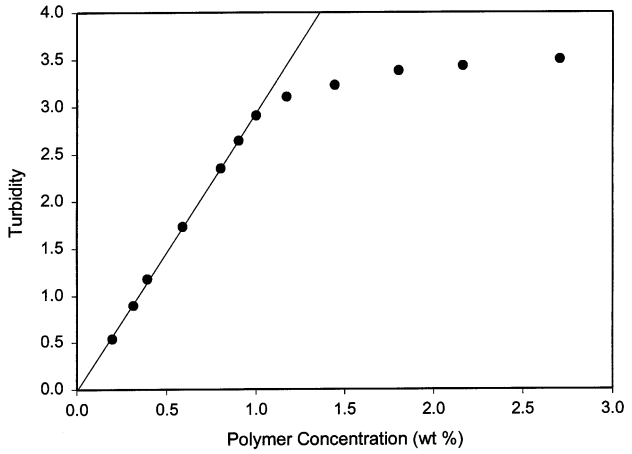

Fig. 1. Dependence of the solution turbidity on the polymer concentration for vesicular aggregates in water. The line illustrates the linear fit at lower concentrations.

concentration is increased. Shen and Eisenberg have shown that approaching the transition region from the vesicle side by adding dioxane to the system results in a decrease in both the mean diameter and the wall thickness of the vesicles [53]. For example, at a solvent composition of 28.0 wt% H_2O, the vesicles have a mean diameter of 87.6 ± 2.3 nm when the polymer concentration is 1.26 wt%; this value changes to 84.3 ± 1.9 nm when the polymer concentration is reduced to 0.72 wt%. When the solvent composition is 40 wt% in water, the mean vesicle diameter is 96.7 ± 2.7 and 90.2 ± 2.1 nm at polymer concentrations of 1.80 and 0.60 wt%, respectively. It must also be noted that an approach to the transition region from the rod zone leads to a decrease in the length and an increase in the diameter of the rods. At the boundary between the rod and the transition region, the average length of a rod is ca. 400 nm and a diameter of ca. 20 nm [67].

It has previously been shown that these dimensional changes are reflected in the solution turbidity, with the turbidity increasing as the aggregates, of a given morphology, grow in size [20]. However, the concentration of the aggregates also affects the solution turbidity. Fig. 1 shows a plot of concentration dependence of the solution turbidity for vesicular aggregates. The vesicles were prepared in a mixture of 30.0 wt% H_2O–70.0 wt% dioxane, but the solution was dialyzed against water to remove the dioxane. This kinetically freezes the aggregates so that they remain as vesicles when the solution is diluted. The plot indicates that there is a linear dependence of turbidity on polymer concentration below ca. 1.0 wt% polymer.

3.2. Interpretation of dimensional and structural changes

The structure of PS_{310}-*b*-PAA_{52} aggregates is affected by the interfacial energy between the aggregate core and the solvent, the repulsive interactions among the corona chains, and the core-chain stretching. It is the balance between these forces that dictates the morphology of the aggregates under a given set of conditions. Perturbing the system with a sudden change in the solvent composition, therefore, alters this equilibrium between the forces, leading to morphological change [20,43–51].

The stability of vesicles prepared from block copolymers, like those composed of lipids or other small amphiphiles, is dependent on the curvature energy [71]. The degree of curvature is determined by the force balance governing the aggregates [53]. Hence, the stability of the vesicles is influenced by the solvent composition of the system. Increasing the dioxane content of the solvent decreases the stretching of the PS blocks in the core of the bilayer and also decreases the repulsive interactions among the corona chains, which leads to a reduction in the interfacial energy between the core and the solvent. These favorable energy changes contribute to a reduction in the mean diameter of the aggregates. However, there is only a slight decrease in the thickness of the bilayer. In order to compensate for this imbalance in the dimensional changes, the degree of vesicle curvature increases. The resulting rise in the curvature energy makes the vesicles unstable; they change their morphology in order to relieve this strain.

3.3. Mechanism of morphological change

The images obtained from the TEM studies suggest that the vesicle-to-rod transition proceeds through a complex, multi-step mechanism. Fig. 2 contains a series of micrographs corresponding to the structural changes that occur during the jump from 29.0 to 26.4 wt% H_2O in a solution

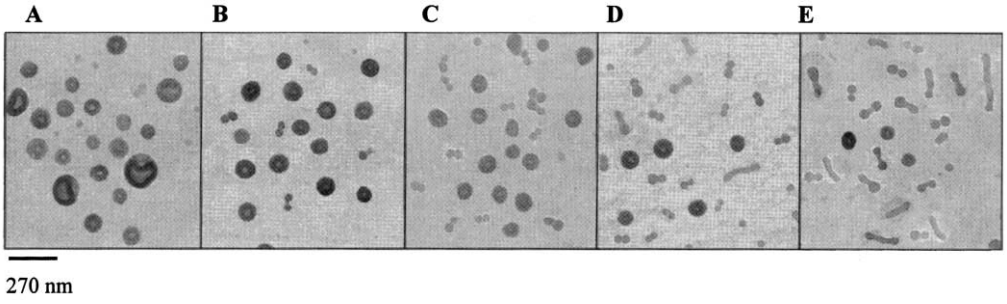

Fig. 2. Micrographs of the aggregate morphologies at various time points during the transition from 29.0 to 26.4 wt% H_2O in a 1.0 wt% PS_{310}-*b*-PAA_{52} solution: (A) 0 s; (B) 5 s; (C) 11 s; (D) 17 s; (E) 25 s).

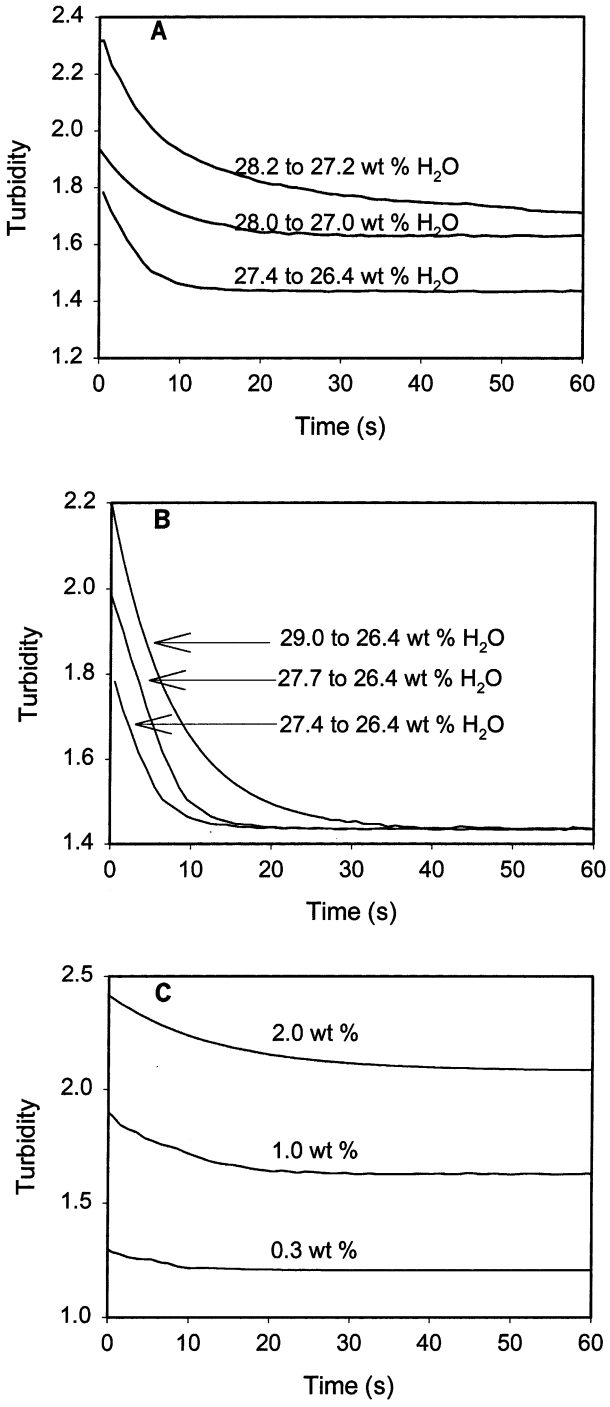

Fig. 3. (A) Effect of the initial solvent composition on the kinetics of the vesicle-to-rod transition in PS_{310}-*b*-PAA_{52} aggregates in dioxane–water mixtures. The initial polymer concentration is 1.0 wt%. (B) Effect of the magnitude of the dioxane jump on the kinetics of the vesicle-to-rod transition in PS_{310}-*b*-PAA_{52} aggregates in dioxane–water mixtures. The initial polymer concentration is 1.0 wt%. (C) Effect of the initial polymer concentration on the kinetics of the vesicle-to-rod transition from 28.0 to 27.0 wt% H_20 in PS_{310}-*b*-PAA_{52} aggregates.

with an initial polymer concentration of 1.0 wt%. The beginning stages of the structural transformation involve a reduction in the mean vesicle diameter of the polydisperse sample and the reorganization of the vesicular structures yielding bowtie-shaped (two spheres in contact) aggregates. Some of the samples (not shown) are shadowed with a Pt/Pd alloy in order to get an indication of the thickness of these aggregates. It is concluded from this study that the bowties are not bilayer structures. The volume of a bowtie (V_b) is approximately equal to that of a vesicle (V_v) ($V_b = 5.1 \pm 0.7 \times 10^5$ nm^3, $V_v = 5.4 \pm 0.5 \times 10^5$ nm^3), although the size distribution of both populations is quite broad. It is not likely that the bowtie aggregates directly result from the collapse of the vesicle. One might speculate that the bowties are actually two small adjoining vesicles; however, no core has ever been observed in these aggregates, and if one did exist, it is estimated, from volume calculations (assuming the wall thickness remains the same), to be approximately 20 nm, which would certainly be observable with TEM. Considering that the aggregates are seen only in two dimensions and that the sample handling procedure prevents us from obtaining micrographs of the first few seconds of the transition, it is likely that there is another intermediate aggregate morphology that appears prior to the bowtie structure. As the transition progresses, the bowties begin to elongate into aggregates resembling dumbbells. The long axis of these aggregates lengthens at the expense of the size of the bulbs on either end. The final rods are ca. 300 nm in length and have a diameter of 25 nm. The vesicles, rods, and intermediate structures are all of similar volume; thus, it is concluded that one vesicle is converted to one rod, as is the case for the rod-to-vesicle transition.

3.4. Transition kinetics

The kinetics of structural transitions in colloidal aggregate systems has most often been studied using relaxation methods utilizing temperature, concentration, and pressure jump techniques [63–67,72]. In this particular study, a jump in the dioxane content of the dioxane–water solvent system is employed to induce the vesicle-to-rod transition in aggregates of PS_{310}-*b*-PAA_{52}. The transformation is followed by monitoring the solution turbidity as a function of time because the turbidity has been shown to be sensitive to changes in the size and shape of the aggregates [20].

All of the turbidity curves associated with this transition have been found to fit best to a single exponential equation.

$$Y = C + Ae^{-t/\tau} \quad (1)$$

where Y is the turbidity, C and A are adjustable parameters, t is the time, and τ is the relaxation time. It is interesting to note that the value of C is equal to the turbidity of the solution at infinite time. The fact that there is a single relaxation time is inconsistent with the details outlined for the transition mechanism. The transformation of vesicle into

Table 1
Kinetic results for vesicle-to-rod transition of PS_{310}-*b*-PAA_{52} aggregates in dioxane/water mixtures

	Initial polymer concentration	Initial H_2O content	ΔH_2O	C	A	τ (s)	R^2
Initial water content	1.01	28.2	− 1.0	1.66	0.465	7.22	0.999
	1.00	28.0	− 1.0	1.63	0.409	6.13	0.999
	1.02	27.6	− 1.0	1.46	0.329	4.72	0.997
	1.01	27.4	− 1.0	1.44	0.309	3.97	0.997
Jump magnitude	1.03	29.0	− 2.6	1.44	0.765	7.86	1.00
	1.01	27.7	− 1.3	1.44	0.584	5.65	0.995
	1.01	27.4	− 1.0	1.44	0.309	3.97	0.997
Polymer concentration	0.30	28.0	− 1.0	1.21	0.093	5.88	0.990
	1.00	28.0	− 1.0	1.63	0.409	6.13	0.999
	2.02	28.0	− 1.0	2.08	0.332	12.8	0.996

rods appears to involve multiple steps beginning with the reduction in the mean diameter of the vesicles, followed by the reorganization of the vesicles to form a non-bilayer bowtie aggregate. These bowties elongate to form rods. As mentioned earlier, the bowtie structure is not a logical step in the evolution in the morphology of the aggregates from the vesicular state because it is unlikely that a spherical bilayer aggregate can collapse to form a non-bilayer aggregate with a bowtie structure. This hypothesis, coupled with the fact that a single relaxation time is obtained for the kinetics of what is obviously a multi-step process, leads to the conclusion that possibly experimental limitations prevent us from detecting the relaxation process of the fastest step(s) in the transition, and that the relaxation time that is obtained corresponds to the expansion of the bow ties in the direction of the long-axis. This conclusion is justified considering the short time scale over which the transition occurs. Because of this uncertainty in the kinetic data, it is more appropriate to discuss the transition in terms of relaxation time instead of simplifying the results in order to obtain a rate constant.

3.5. Factors effecting the transition kinetics

3.5.1. The initial solvent composition

Fig. 3A contains turbidity–time profiles for the vesicle-to-rod transition induced at different solvent compositions; they suggest that this parameter of the system has a slight influence on the transition kinetics. This effect was studied by applying a 0.5 wt% jump in the dioxane content to a series of solutions with different solvent compositions, and with a 1.0 wt% polymer concentration. The starting position was varied from 28.2 to 27.4 wt% H_2O. The relaxation times increase with an increase in the initial water content (Table 1). This phenomenon must be considered in terms of where the initial conditions place the system within the morphological phase diagram. At 28.2 wt% H_2O, the system is located within the vesicle region and is further away from the transition boundary than the starting position of any other experiment. The kinetics is slower for this transition because all the aggregates are equilibrium vesicles, thus the aggregates must undergo a larger degree of structural rearrangement as they progress toward rods, than those systems (i.e. 27.6 and 27.4 wt% H_2O) that start out already within the transition region. The mean vesicle diameter increases with increasing water content in the solvent, but the wall thickness is relatively constant [18]. This indicates that the hollow regions of the vesicles are able to hold more solvent. Hence, the kinetics progressively slow down with increasing initial water content because more solvent must be expelled from the vesicle core in order for it to reorganize to become a non-bilayer aggregate.

The relaxation times for the rod-to-vesicle transition also increase with increasing water content [67]. This is attributed to the fact that the slow step in the transition, the closure of the lamellae or bowls to form vesicles, contributes more to the turbidity change than the fast initial formation of the lamellae from rods at higher water contents. It is noteworthy that the rod-to-vesicle transition occurs much more slowly than the opposite, vesicle-to-rod transition in spite of the fact that it is induced at higher water contents. A high ratio of water to dioxane in the solvent can kinetically trap the morphology of the aggregates by affecting the mobility of the copolymer chains. This factor does not influence the kinetics of the transitions because the difference in the starting solvent composition between the forward and reverse transitions is small relative to the composition range covered by the morphological phase diagram.

3.5.2. The size of the dioxane content jump

Altering the solvent composition effects, the force balance governing the aggregate morphology, and is used to drive the morphological transition. In order to gain a better understanding of the vesicle-to-rod transition, it is important to determine how the degree of perturbation imposed on the system influences the transition kinetics. This is accomplished by applying different dioxane content jumps, ranging from 1.0 to 2.6 wt%, to solutions with a polymer concentration of 1.0 wt% (Fig. 3B). The initial solvent composition is varied, depending on the size of

the jump, so that the final solvent composition is 26.4 wt% H_2O–73.6 wt% dioxane in all cases.

The relaxation time becomes slightly longer with an increase in the magnitude of the dioxane jump as outlined in Table 1. This result is attributed to the initial conditions of the system, and the location of each system within the phase diagram. Since the drive is toward the formation of rods, it will take longer to reach this desired state the further the system resides to the right of the transition region because the aggregates must proceed through more structural rearrangement steps and more solvent must be expelled from the core of the vesicles before they begin to resemble rods. At water contents above 28.0 wt%, the vesicles are considered to be equilibrium structures. Thus, the bigger the magnitude of the perturbation imposed on these aggregates, the farther they are driven away from their initial equilibrium state, and the longer it takes for the aggregates to reach a new state of equilibrium.

The kinetics of the rod-to-vesicle transition, like that of the vesicle-to-rod transition, has a slight dependence on the magnitude of the solvent jump. Chen et al. argue that the reason for this result is that the Gibbs activation energy is not strongly influenced by the size of the solvent jump [67]. However, there is a very large difference in the relaxation times for these opposing transitions, with the vesicle-to-rod transition occurring more quickly than the reverse transition when the same degree of perturbation is applied to both systems.

3.5.3. The initial polymer concentration

By keeping the solvent composition and the size of the dioxane jump constant, it is possible to explore the effect that the initial polymer concentration has on the kinetics of the transition. Fig. 3C contains turbidity curves for three systems with polymer concentrations ranging from 0.3 to 2.0 wt%. A 1.0 wt% jump in the dioxane content is used to induce the transition.

The relaxation time for the transition becomes longer as the polymer concentration is increased. The effect is more pronounced at higher polymer concentration; there is a twofold increase in the value of τ in going from 1.0 to 2.0 wt% PS-*b*-PAA. The phase diagram studies indicate that the transition boundaries are shifted to lower water content with increasing polymer concentrations. The boundary between the vesicle and transition regions is situated at a solvent composition of ca. 24.0 wt% H_2O when the polymer concentration is 2.0 wt%. This is increased to 27.6 wt% and ca. 28.5 wt% for polymer concentrations of 1.0 and 0.3 wt%, respectively. Hence, the starting conditions place the system within the vesicle region when the polymer concentration is 1.0 and 2.0 wt%, but within the transition region when the polymer concentration is 0.3 wt%. The mean diameter of the vesicles also increases with a rise in the polymer concentration, but the bilayer thickness remains constant. Thus, not only are the aggregates initially all vesicles at 2.0 wt% polymer, but they also contain a larger amount of solvent in their core. The transition kinetics are slower at higher polymer concentrations because the systems is deeper within the vesicle regions, causing the aggregates to have to undergo more reorganization, and expel more solvent from the core in order for them to become non-bilayer structures. There is only a slight difference in the relaxation times in going from 0.3 to 1.0 wt% polymer. The initial parameters place these systems approximately the same distance away, but on opposite sides of the transition boundary, so their starting conditions are more closely related than those at 2.0 wt% polymer. The same trend is observed for the effect of the initial polymer concentration on the rod-to-vesicle transition. Chen et al. attribute this to an increase in the activation energy with increasing polymer concentrations [67].

3.6. Comparison of the results with those of other PS-b-PAA aggregate transitions

To date, the kinetics and mechanism of four morphological transitions that occur in aggregates prepared from PS_{310}-*b*-PAA_{52} in dioxane–water mixtures have been investigated [67,68]. These include the sphere-to-rod, the rod-to-sphere, the rod-to-vesicle, and the vesicle-to-rod transitions. Although the exact mechanistic details are different for each transition, the morphological transformations can be compared in terms of the kinetics and the more fundamental aspects of the transition process. The accumulation of this information can lead to better insight into how to control the morphology of the block copolymer aggregates. A complete understanding of the morphological behavior of block copolymer aggregates is useful not only for its own sake, but also if these aggregates are to be employed in potential applications in such areas as pharmaceuticals, agriculture, and personal care products.

The sphere-to-rod transition proceeds through a two-step mechanism [68]. As the transition boundary is approached, the spherical micelles become energetically unstable because of core-chain stretching. This results in the adhesive collisions between the spheres leading to 'pearl necklace' formation in order to reduce the energy of the system. During the rate-determining step, the individual chains within a necklace reorganize to produce a smooth rod with a smaller diameter than that of the original spherical aggregates. The reverse transition, rod-to-sphere, also has a two-step mechanism [68]. In this case, a bulb quickly grows on one or both ends of a rod. The bulbs are extruded from the rod to release free spheres during the rate-limiting step.

An increase in the water content of the solvent within the rod region leads to the shortening of the length of the rods accompanied by an increase in the diameter [67]. A sudden jump in the water content near this transition boundary initiates the transformation of rods into vesicles beginning with the flattening of the rods to form circular or irregular shaped lamellae. The lamellae then slowly become

Table 2
General trend in the relaxation times

Transition	General trend in the relaxation time(s)		
	↑ Water content	↑ Jump magnitude	↑ Polymer concentration
Sphere-to-rod	Increase	Decrease	Decrease
Rod-to-sphere	Increase	Increase	Decrease
Rod-to-vesicle	Increase	Slight decrease	Increase
Vesicle-to-rod	Slight increase	Slight increase	Increase

bowl-shaped, and eventually close to form vesicles. As discussed earlier, the vesicle-to-rod transition has a more complex mechanism for which not all of the details are clear. However, the transformation appears to progress from small vesicles to non-bilayer aggregates with a bowtie shape. Growth occurs at the ends of these aggregates to form dumb-bell structures. The expansion of the long-axis continues at the expense of the bulbs on either end until a smooth rod is formed.

The above description of the transition mechanisms reveals two trends in the results. The forward and reverse transition between rods and vesicles both occur without a change in the aggregation number; one rod is converted to one vesicle and vice versa. On the other hand, the sphere-to-rod and rod-to-sphere transitions both proceed without conservation of aggregate mass in that many spheres form one rod. It is also noteworthy that the mechanism of three of the four transitions involves only two transformation steps. Despite this fact, the transition kinetics is as easily compared.

Examining the kinetic results for the forward and reverse transition between two aggregate morphologies indicates that the relaxation times for the sphere-to-rod and rod-to-sphere transitions are of the same order of magnitude, but in the case of rods and vesicles, the relaxation time for the vesicle-to-rod transition is two orders of magnitude shorter than the τ values for the rod-to-vesicle transition. Although the turbidity–time profiles for most of the kinetic experiments are fitted to the same double exponential equation, all of those for the vesicle-to-rod and one experiment from both the sphere-to-rod and rod-to-sphere transition studies yield a single exponential equation.

Table 2 contains a summary of the effect of varying the initial solvent composition, the magnitude of the solvent jump, and the initial polymer concentration on the general trend in the relaxation times for each transition. In all cases, the relaxation times become longer with an increase in the water content of the solvent mixture. This phenomenon is related to the location that each set of parameters places the system within the morphological phase diagram and how this position impacts the progress of the transition. The size of the solvent jump has the opposite effect on the relaxation times of the forward and reverse transitions for both types of morphological transformations, but the trend is the same in both cases. Increasing the size of the water content jump leads to slightly faster kinetics for both the sphere-to-rod and rod-to-vesicle transitions, while increasing the magnitude of the dioxane content jump leads to longer relaxation times for the reverse processes. This result must be considered in terms of the experimental design. For those transitions induced by a jump in the water content, the initial solvent composition was held constant, but for those transitions induced with dioxane, the final solvent composition was constant. The copolymer concentration has a strong influence on the kinetics of morphological change. However, the explanation of the observed trends is more complex. The relaxation times decrease with an increase in the polymer concentration during the sphere-to-rod and rod-to-sphere transitions. However, the relaxation times become longer with higher polymer concentration for the other two transitions. These results are related to both the change in the activation energy for the morphological change and the transition boundaries with varying polymer concentration.

This series of studies of the kinetics and mechanisms of morphological transitions in block copolymer aggregates in solution represents the most extensive investigation of its kind for copolymer systems. However, the complex and diverse nature of the morphological changes in block copolymer aggregates warrants further study in order to completely understand such phenomena.

4. Conclusions

The kinetics and mechanism of the vesicle-to-rod transition has been examined in aggregates systems prepared from the ternary system PS_{310}-*b*-PAA_{52}/dioxane/water. The transition was induced by a jump in the dioxane content of the solvent mixture and was followed by monitoring the solution turbidity as a function of time. A single relaxation time was obtained from the turbidity–time curves. The mechanism was investigated by rapidly quenching to low temperature and subsequently freeze-drying solution samples at various time points during the transitions. This traps the intermediate aggregate morphologies, which are observed using TEM. Approaching the transition boundary from the vesicle region results in a decrease in the mean diameter of the vesicles with little change in the bilayer thickness. This increases the degree of curvature of both

the inner and outer vesicle bilayers leading to an increase in the curvature energy. The instability of these vesicles causes them to undergo structural rearrangement. The first intermediate structure observed is of a bowtie shape. The bowties grow to develop into dumbbells. The long-axis expands at the expense of the bulbs on either end of the dumbbells resulting in the formation of rods. The reduction in the stretching of the core-chains in going from vesicles to rods is expressed in the smaller diameter of the rods relative to that of the bilayer. It is concluded based upon the fact a single relaxation time was obtained for the kinetics of the multi-step transition and that bowties, which do not likely form directly from vesicles, are the first intermediate structures observed, that one or more steps in the transition are not detected as a result of experimental limitations. In any event, the kinetics of the transition is influenced by the initial solvent composition, the magnitude of the dioxane content jump, and the initial polymer concentration. The relaxation time becomes slightly longer with an increase in both the water content of the solvent mixture and the degree of solvent perturbation. The kinetics has a greater dependence on the polymer concentration than the other two parameters investigated.

Acknowledgements

This work was supported by funding from the Natural Sciences and Engineering Research Council of Canada (NSERC). SEB is grateful for scholarship funding provided by NSERC. We would like to thank Dr H. Shen for synthesizing the polymer.

References

[1] Price C, Woods D. Eur Polym J 1973;9(8):827–33.
[2] Tuzar Z, Kratochvil P. Adv Colloid Interf Sci 1976;6(3):201–32.
[3] Price C. In: Goodman I, editor. Developments in block copolymers, vol. 1. London: Applied Science Publishers, 1982. p. 39.
[4] Elis HG. In: Huglin MB, editor. Light scattering from polymer solutions. London: Academic Press, 1972. Chapter 9.
[5] Riess G, Hurtrez G, Bahadur P. Encyclopedia of polymer science and engineering. 2nd ed, vol. 2. New York: Wiley, 1985 p. 324.
[6] Selb J, Gallot Y. In: Goodman I, editor. Developments in block copolymers, vol. 2. London: Applied Science Publishers, 1985. p. 27.
[7] Brown RA, Masters AJ, Price C, Yuan XF. In: Allen SG, Bevington JC, Booth C, Price C, editors. Comprehensive polymer science: polymer properties, vol. 2. Oxford: Pergamon Press, 1989. p. 155.
[8] Tuzar Z, Kratochvil P, Matijievic E, editors. Surface and colloid science, vol. 15. New York: Plenum Press, 1993. p. 1.
[9] de Gennes PG. In: Liebert L, editor. Solid state physics. New York: Academic Press, 1978. p. 1, suppl. 14.
[10] Halperin A, Tirrell M, Lodge TP. Adv Polym Sci 1992;100:31–71.
[11] Bednar B, Edwards K, Almgren M, Tormod S, Tuzar Z. Makromol Chem Rapid Commun 1988;9(12):785–90.
[12] Honda C, Hasegawa Y, Hirunuma R, Nose T. Macromolecules 1994;27(26):7660–8.
[13] Hecht E, Hoffmann H. Colloid Surf A: Physiochem Engng Aspects 1995;96(1/2):181–97.
[14] Iyama K, Nose T. Macromolecules 1998;31(21):7356–64.
[15] Michels B, Waton G, Zana R. Langmuir 1997;13(12):3111–9.
[16] Aniansson EAG, Wall SN. J Phys Chem 1974;78(10):1024–30.
[17] Zhang L, Eisenberg A. Science 1995;268(5218):1728–31.
[18] Shen H, Eisenberg A. J Phys Chem B 1999;103(44):9473–87.
[19] Yu K, Eisenberg A. Macromolecules 1998;31(11):3509–18.
[20] Zhang L, Eisenberg A. Polym Adv Tech 1998;9(10–11):677–99.
[21] Cameron NS, Corbierre MK, Eisenberg A. Can J Chem 1999;77(8):1311–26.
[22] Burke S, Eisenberg A. High Perform Polym 2000;12(4):535–42.
[23] Ding J, Liu G. Polymer 1997;38(21):5497–502.
[24] Hajduk DA, Kossuth MB, Hillmyer MA, Bates FS. J Phys Chem B 1998;102(22):4269–76.
[25] Discher BM, Won YY, Ege DS, Lee JCM, Bates FS, Discher DE, Hammer DA. Science 1999;284(5417):1143–6.
[26] Prochazka K, Martin TJ, Webber SE, Munk P. Macromolecules 1996;29(20):6526–30.
[27] Spatz JP, Mössmer S, Möller M. Angew Chem Int Ed Engl 1996;35(13/14):1510–2.
[28] Massey J, Power KN, Manners I, Winnik MA. J Am Chem Soc 1998;120(37):9533–40.
[29] Kramer E, Förster S, Goltner C, Antonietti M. Langmuir 1998;14(8):2027–31.
[30] Jørgebseb EB, Hvidt S, Brown W, Schillén K. Macromolecules 1997;30(8):2355–64.
[31] Liu G. Curr Opin Colloid Interf Sci 1998;3(2):200–8.
[32] Liu T, Zhou Z, Wu C, Chu B. J Phys Chem B 1997;101(43):8808–15.
[33] Mortensen K, Talmon Y, Gao B, Kops J. Macromolecules 1997;30(22):6764–70.
[34] Yu Y, Eisenberg A. J Am Chem Soc 1997;119(35):8383–4.
[35] Rheingans O, Hugenberg N, Harris JR, Fischer K, Maskos M. Macromolecules 2000;33(13):4780–90.
[36] Alexandridis P, Olsson U, Lindman B. Langmuir 1998;14(10):2627–38.
[37] Yu K, Zhang L, Eisenberg A. Langmuir 1996;12(25):5980–4.
[38] Svensson M, Alexandridis P, Linse P. Macromolecules 1999;32(3):5435–45.
[39] Svensson B, Olsson U, Alexandridis P. Langmuir 2000;16(17):6839–46.
[40] Desbaumes L, Eisenberg A. Langmuir 1999;15(1):36–38.
[41] Mortensen K, Pedersen JS. Macromolecules 1993;26(4):805–12.
[42] Schillén K, Brown W, Johnsen RM. Macromolecules 1994;27(17):4825–32.
[43] Zhang L, Yu K, Eisenberg A. Science 1996;272(5269):1777–9.
[44] Zhang L, Shen H, Eisenberg A. Macromolecules 1997;30(4):1001–11.
[45] Shen H, Zhang L, Eisenberg A. J Am Chem Soc 1999;12(12):2728–40.
[46] Talingting MR, Munk P, Webber SE, Tuzar Z. Macromolecules 1999;32(5):1593–601.
[47] Jørgebseb EB, Hvidt S, Brown W, Schillén K. Macromolecules 1997;30(8):2355–64.
[48] Kabanov AV, Bronich TK, Kabanov VA, Eisenberg A. J Am Chem Soc 1998;120(38):9941–2.
[49] Zheng Y, Davis HT. Langmuir 2000;16(16):6453–9.
[50] Shen H, Zhang L, Eisenberg A. J Phys Chem B 1997;101(24):4697–708.
[51] Zhang L, Eisenberg A. Macromolecules 1999;32(7):2239–49.
[52] Shen H, Eisenberg A. Macromolecules 2000;33(5):2561–72.
[53] Luo L, Eisenberg A. J Am Chem Soc 2001;123(5):1012–3.
[54] Yu K, Bartels C, Eisenberg A. Langmuir 1999;15(21):7157–67.
[55] Schillén K, Bryskhe K, Mel'nikova YS. Macromolecules 1999;32(20):6885–8.
[56] Koňák C, Oupický D, Chytrý V, Ulbrich K. Macromolecules 2000;33(15):5318–20.
[57] Vinson PK, Talmon Y, Walter A. Biophys J 1989;56(4):669–81.
[58] Walter A, Vinson PK, Kaplun A, Talmon Y. Biophys J 1991;60(6):1315–25.

[59] Edwards K, Almgren M. J Colloid Interf Sci 1991;147(1):1–21.
[60] Edwards K, Almgren M, Bellare J, Brown W. Langmuir 1989;5(2):473–8.
[61] Edwards K, Gustafsson J, Almgren M, Karlsson G. J Colloid Interf Sci 1993;161(2):299–309.
[62] Silvander M, Karlsson G, Edwards K. J Colloid Interf Sci 1996;179(1):104–13.
[63] Farquhar KD, Misran M, Robinson BH, Steytler DC, Morini P, Garrett PR, Holzwarth JF. J Phys Condens Matter 1996;8(47):9397–404.
[64] Danino D, Talmon Y, Zana R. J Colloid Interf Sci 1997;185(1):84–93.
[65] Brinkmann U, Neumann E, Robinson BH. J Chem Soc Faraday Trans 1998;94(9):1281–5.
[66] Iyama K, Nose T. Macromolecules 1998;31(21):7356–64.
[67] Chen L, Shen H, Eisenberg A. J Phys Chem B 1999;103(44):9488–97.
[68] Burke SE, Eisenberg A., submitted to Langmuir.
[69] Hautekeer JP, Varshney SK, Fayt R, Jacobs C, Jerome R, Teyssie P. Macromolecules 1990;23(17):3893–8.
[70] Zhong XF, Varshney SK, Eisenberg A. Macromolecules 1992;25(26):7160–9.
[71] Inoue T. Vesicles. In: Rosoff M, editor. Surfactant science series, vol. 62. New York: Marcel Dekker, 1996. Chapter 5.
[72] Aniansson EAG, Wall SN, Almgren M, Hoffmann H, Kielman I, Ulbricht W, Zana R, Lang J, Tondre C. J Phys Chem 1976;80(9):905–22.